Substrate Effects in Squeeze Film Damping of Lateral Parallel-Plate Sensing MEMS Structures

Axel Berny, *Student Member, IEEE*

Abstract— **Squeeze film damping is a major source of noise in MEMS structures. Since damping limits the sensing accuracy of a given MEMS structure, a model relating design parameters to the damping coefficient is critical so that the system may be optimized. Several successful squeeze-film damping models exist [1-3]. While certain models are able to accommodate complicated edge effects [2] and perforations [3], to the best of our knowledge, none have addressed substrate proximity effects. This paper introduces a simplified squeeze-film macro-model for a lateral parallel-plate sensing structure (Fig. 1) that takes into account substrate proximity effects. Second order considerations such as edge effects, compressibility effects, Couette flow damping (between the substrate and the laterally moving mass), and non-zero slip conditions are not included here as they have been successfully addressed elsewhere [1-4]. Substrate proximity effects are approximated by modeling the gap separating the mass and substrate as a channel. Despite its many simplifications, our model delivers sufficient accuracy for hand-analysis as needed during initial design steps. Our results were validated against simulations obtained via the *CoventorWare MemDamping* module.**

Index Terms—**Damping model, Squeeze film, Viscous Damping.**

I. INTRODUCTION

D amping is a critical consideration in the design of many planar MEMS devices such as accelerometers and gyroscopes. While Couette-type damping models typically take into account the interaction between a substrate layer and a moving mass [4], present squeeze-film damping models do not. The main motivation of this research stemmed from the fact that squeeze-film damping is affected by the substrate in many common situations. As illustrated in Fig. 1, the substrate tends to constrict the air being squeezed out of the gap. If the gap in question is located sufficiently close to the substrate, the pressure gradient between the two plates is directly affected. In modern MEMS processes, the distance separating a metal/poly layer and the substrate is
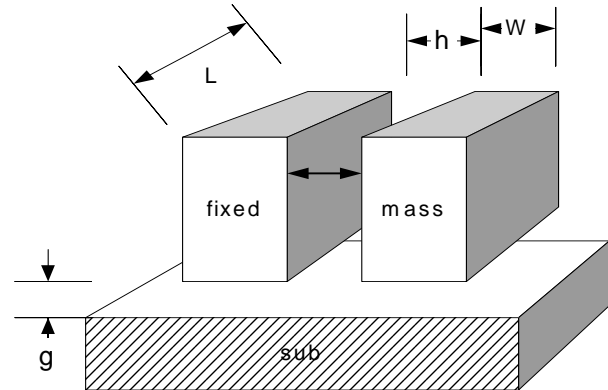
Fig. 1. Typical lateral parallel-plate sensing structure.

typically between 1 and 10μm. Hence such effects can easily contribute non-negligible damping components.

Section II of this paper begins with a treatment of some of the established theory describing squeeze-film damping. This is then used as the foundation for our modeling of substrate proximity effects. Several secondary modeling considerations (treated elsewhere) are discussed to provide the reader with a practical sense of what must be assessed in order to achieve accurate predictions of squeeze-film damping effects.

In section III, simulation results are presented and compared to hand-analysis models derived in the previous section.

II. SQUEEZE-FILM DAMPING

A. Basic Theory

In general, Navier-Stokes equations describe viscous, pressure, and inertial mechanisms in fluids. Under certain flow conditions, these much-complicated Navier-stokes equations can be simplified into the Reynolds equations. Its underlying assumptions are as follows: 1) the film is isothermal, 2) inertial effects are negligible, 3) amplitude motion and pressure changes are small, 4) fluid velocity normal to the surface is negligible, and 5)

the gap is small compared to lateral dimensions ($h_o \ll L, W$).

The isothermal *Reynolds* equation is:

$$\frac{\partial}{\partial h} \cdot \left(PH^3 \frac{\partial P}{\partial h} \right) = \sigma \frac{\partial (PH)}{\partial t}, \qquad (1)$$

with $P = \Delta p / P_o$ and $\sigma = 12\mu L^2 / (P_o h_o^2)$, and where P is the normalized pressure, Δp is the small variation in pressure, P_o is the ambient pressure, H is the normalized gap thickness h/h_o, μ is the fluid viscosity, and L is the length of the moving mass.

B. Secondary Considerations

1) Continuum Limits

Both Navier-Stokes and Reynolds are derived under the assumption that the fluid medium is continuous, implying that energy transfer is only achieved through molecular interaction within the fluid. This condition is only satisfied when the ratio of the fluid particle mean free path to the characteristic dimension of the system is less than one tenth or so. Violation of this condition leads to non-zero slip-conditions (momentum is transferred as fluid molecules collide with the oscillating plates), which in turn results in a higher fluid flow rate and a reduced damping coefficient. This effect can be modeled by an effective viscosity given in [8]:

$$\mu_{eff} = \frac{\mu}{1 + 9638 \left(\frac{P_o}{P} \cdot \frac{\lambda}{L} \right)^{1.159}}. \qquad (2)$$

2) Edge-effects

Finite element simulations have been used to take effects due to finite size, edges, and perforations [2, 3]. As pointed out in [2], the use of trivial boundary conditions where the gauge pressure is set to zero at edges leads to large errors, especially as plate dimensions decrease (see Fig. 5 in [2]). This deficiency steams from the fact that the gauge pressure become zero only at a certain distance away from any edge. The authors in [2] demonstrated that applying trivial boundary conditions to a control volume that extends beyond the plate edges yields accurate (simulation) results.

3) Compressibility and squeeze number

In squeeze-film analysis, it is common to introduce a non-dimensional squeeze number defined [1,3,5] as:

Fig. 2. Squeeze-film damping setup.

$$\sigma = \frac{12\mu\omega L^2}{h_o^2 P_o}, \qquad (3)$$

where ω is the oscillation frequency. For squeeze numbers less than 0.2 [1], the gas behaves as if it were incompressible. Otherwise, the film stiffness increases as the squeeze number increases and the damping coefficient falls approximately as $1/\sigma^{0.4}$ [5].

C. Substrate Proximity Effects

For the sake of clarity/simplicity, let us consider the case where Reynolds equations apply. Furthermore, let us limit our analysis to geometries for which a 1-dimensional flow dominates ($L \gg W$). This is only a modest restriction since this condition is satisfied for many structures such as ADI's ADXL50 [6]. In addition, low excitation frequencies are assumed so that the term $\partial P / \partial t$ in (1) can be set to zero. Hence equation (1) is linearized as follows:

$$\frac{\partial^2 P(x)}{\partial x^2} = \frac{12\mu}{h_o^3} \cdot \frac{\partial h}{\partial t}, \qquad (4)$$

where $P(x)$ is the pressure departure from the nominal ambient pressure P_o, as a function of x. The above differential equation is the basis of our analysis and is applied to regions 1 and 2 of Fig. 2. Note that for region 2, the right hand-side vanishes since the term $\partial h / \partial t$ is effectively zero. First, we solve for the damping coefficient without considering the presence of the substrate (i.e. $g_o \rightarrow \infty$).

Integrating twice and applying boundary conditions, we get the following pressure profile:

$$P(x) = \frac{12\mu}{h^3} \cdot \frac{\partial h}{\partial t} \cdot \left(\frac{x^2}{2} - \frac{W}{2} x \right). \quad (5)$$

Integrating $P(x)$ over the plate area $A_1=LW$ (which yields the damping force) and dividing by $\partial h/\partial t$, we get the damping coefficient:

$$b = -\frac{\mu}{h_o^3} \cdot LW^3, \quad (6)$$

Next let us bring the substrate into the picture. Since the presence of the substrate restricts the air flow out of the bottom side of the actuator gap, it has a direct impact on the pressure profile *within* the gap. For simplicity, the volume of space between the bottom of the plates and the substrate (region 2 in Fig. 2) is approximated as a channel of cross-section area $A_2 = g_o L$ and length $d_o = d + h_o/4$, extending in the x-direction (the change in direction of the flow is neglected).

Integrating (5) twice, we obtain:

$$P_1(x) = \frac{12\mu}{h_o^3} \cdot \frac{\partial h}{\partial t} \cdot \frac{x^2}{2} + C_1 \cdot x + C_0 \quad (7a)$$

$$P_2(x) = D_1 \cdot x + D_0 \quad (7b)$$

where $P_1(x)$ and $P_2(x)$ are the pressure profiles in regions 1 and 2, respectively. C_1, C_0, D_1, and D_0 are integration constants to be determined by applying appropriate boundary conditions. In the case where the substrate is absent, the pressure gradient is zero at the center of the plates ($x=W/2$) and an ideal boundary can be assumed (no edge effects) where the gas pressure settles to ambient at the edges of the plates ($P_1(0)=P_1(W)=0$). However in our case, most of the aforementioned boundary conditions no longer hold. While $P_1(0)=0$ still holds, new boundary conditions must be established at the interface of regions 1 and 2. The following boundary conditions are determined:

$$P_2(W + d_o) = 0, \quad (8a)$$

$$A_1 \cdot \frac{\partial P_1(W)}{\partial x} = A_2 \cdot \frac{\partial P_2(W)}{\partial x}. \quad (8b)$$

Substituting back into equation (7a), we get:

$$P_1(x) = \frac{12\mu}{h_o^3} \cdot \frac{\partial h}{\partial t} \cdot \left[\frac{x^2}{2} - Wx + \frac{g_o W^2}{t_o h_o + 2 g_o W} \right] \quad (9)$$

Again we obtain the damping coefficient by integrating the above over the plate area and then dividing by $\partial h/\partial t$:

$$b = \frac{\mu \cdot L}{h_o^3} \cdot \left[4W^3 - 6 \frac{W^4}{2W + {t_o h_o}/{g_o}} \right] \quad (10)$$

From equation (10) above we make the following observations. First, letting $g_o \rightarrow \infty$, equation (10) reduces to equation (5) where the substrate was considered infinitely far away. Next, we note that as the closer the substrate is to the moving plates (g_o decreases) the higher the damping coefficient. This makes sense since increasingly restricting the flow from underneath the moving plates clearly raises the pressure within the gap. Finally, letting $g_o \rightarrow 0$, (10) yields a damping coefficient exactly 4 times greater than for the case where the substrate is absent (see equation (5)). These results are verified via simulations in the following section. Equation (10) is plotted in Fig. 3 as a function of g_o for various dimensions.
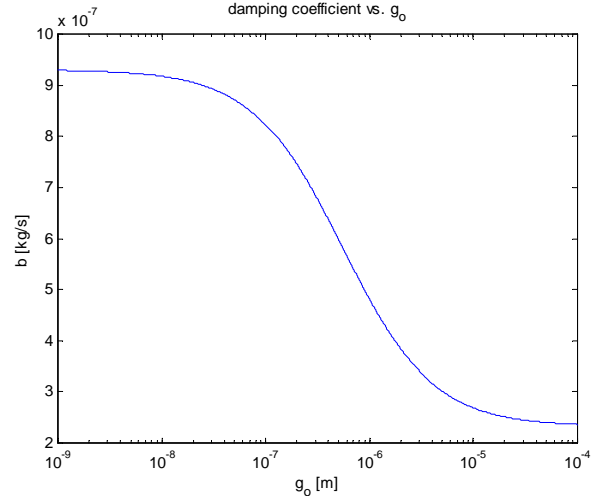
Fig.3. Plot of equation (10) as a function of g_o.

III. SIMULATION RESULTS

In an attempt to verify our model derived above, we simulated a typical structure as shown in Fig. 1. Our simulation tool is a damping module from the MEMS CAD package *CoventorWare* (formerly *MEMCAD*). Finding an adequate simulator for this type of problem is a non-trivial task. The *CoventorWare* package was chosen since it was the only know tool having an actual squeeze-film damping simulation engine. However, it was discovered too far along the way that this tool cannot take neighboring structures (e.g. a substrate plane nearby) into account for such simulations. Despite this serious limitation, extreme cases where the substrate is moved infinitely close or infinitely far away were successfully verified (since these special cases can be modeled by applying appropriate boundary conditions). Fig. 4 displays hand calculations based on equation (10), superimposed by simulation results. Fig. 5 shows the percent error between equation (10) and finite-element simulations, as a function of the plate's lateral dimension (*L*). As expected, (10) is no longer valid for lengths on the order of the plate's vertical dimension (*W*). This is because (10) assumes a very long and narrow strip (*L*>>*W*) such that the gas flow can be approximated as unidirectional (*x*-direction in the above derivation).

IV. CONCLUSIONS

We have investigated substrate proximity effects on squeeze-film damping in a generic lateral parallel-plate sensing MEMS structure. Our simplified model derived in Section II shows excellent agreement with finite-element simulations for long and narrow structures where a 1-D gas flow dominates. The exact same approach can be applied to derive a 2-D (x-y) model. Hence, despite its many simplifying assumptions, the proposed model reasonably predicts squeeze-film damping between two plates suspended above a substrate layer and is particularly well suited for hand-analysis during the initial phases of a design.

V. ACKNOWLEDGMENTS

The author would like to thank Xuesong Jiang for suggesting this project topic and for sharing his knowledge in many helpful discussions throughout the course of this research.

VI. REFERENCES

[1] J. B. Starr, "Squeeze Film Damping in Solid State Accelerometer", Tech. Digest, IEEE Solid State Sensor and Actuator Workshop, USA, June 1990, pp. 44-47.
[2] S. Vemuri, G. K. Fedder, and T. Mukherjee, "Low-Order Squeeze Film Model for Simulation of MEMS Devices", 2000 International Conference on Modeling and Simulation of Microsystems, March 27-29, US Grant, San Diego, pp. 206-208.
[3] E. S. Kim, Y. H. Cho, and M. U. Kim, "Effect of holes and edges on the squeeze film damping of perforated micro-mechanical structures", IEEE *Int. Conf. MEMS*, 1999, pp. 296-301.
[4] Y-H. Cho, A.P. Pisano, and R.T. Howe, "Viscous Damping Model for Laterally Oscillating Microstructures", Journal of Microelectromechanical Systems, Vol. 3, No.2, June 1994, pp. 81-87.
[5] M. Andrews, I. Harris, and G. Turner, "A comparison of squeeze-film theory with measurements on a microstructure", *Sensors and Actuators*, A36, 1993, 79-87.
[6] W. Kuehnel, "Modelling of the mechanical behaviour of a differential capacitor acceleration sensor", *Sensors and Actuators*, A48, 1995, 101-108.
[7] M. A. Lemkin, "Micro Accelerometer Design with Digital Feedback Control", Ph.D. Dissertation, University of California, Berkeley, 1997.
[8] CoventorWare, "*Analyzer*TM Supplemental Tutorials and Reference Guide", Section 6.3, M6-14-M6-21.
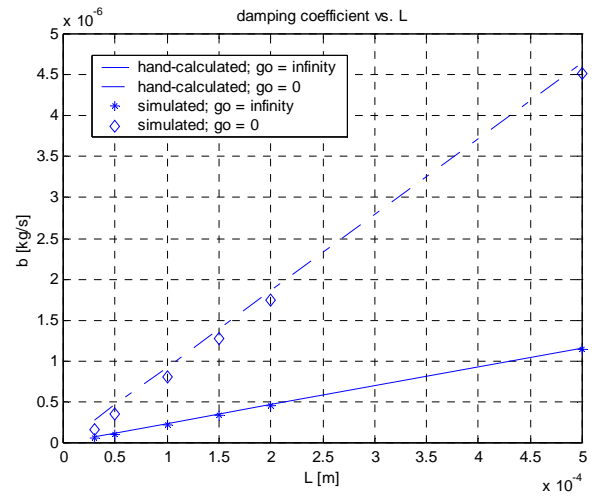
Fig. 4. Hand-calculated and simulated damping coefficients.
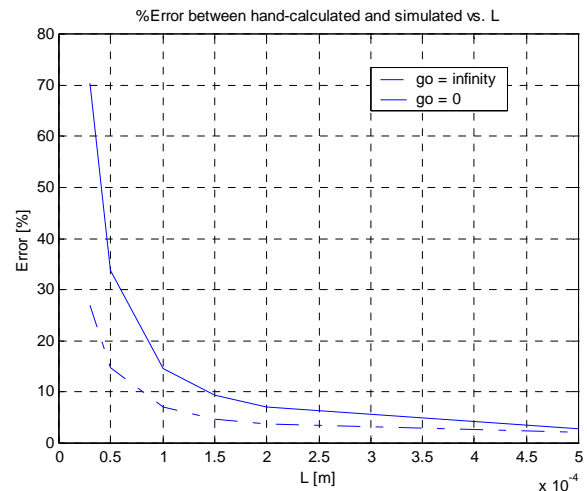
Fig. 5. %Error between hand-calculated and simulated damping coefficients.